

PAPER

Movable shark scales act as a passive dynamic micro-roughness to control flow separation

To cite this article: Amy W Lang *et al* 2014 *Bioinspir. Biomim.* **9** 036017

View the [article online](#) for updates and enhancements.

Related content

- [Experimental study of laminar and turbulent boundary layer separation control of shark skin](#)
Farhana Afroz, Amy Lang, Maria Laura Habegger *et al.*
- [Bristled shark skin: a microgeometry for boundary layer control?](#)
A W Lang, P Motta, P Hidalgo *et al.*
- [Separation control over a grooved surface inspired by dolphin skin](#)
Amy W Lang, Emily M Jones and Farhana Afroz

Recent citations

- [Experimental study of laminar and turbulent boundary layer separation control of shark skin](#)
Farhana Afroz *et al*
- [Direct numerical simulation of sharkskin denticles in turbulent channel flow](#)
A. Boomsma and F. Sotiropoulos
- [Discovery of riblets in a bird beak \(Rynchops\) for low fluid drag](#)
Samuel Martin and Bharat Bhushan

Movable shark scales act as a passive dynamic micro-roughness to control flow separation

Amy W Lang¹, Michael T Bradshaw¹, Jonathon A Smith¹,
Jennifer N Wheelus¹, Philip J Motta², Maria L Habegger² and
Robert E Hueter³

¹Department of Aerospace Engineering & Mechanics, University of Alabama, 255H. M. Comer, 245 7th Avenue, Box 870280, Tuscaloosa, AL 35487, USA

²Department of Integrative Biology, University of South Florida, 4202 East Fowler Avenue, Tampa, FL 33620, USA

³Center for Shark Research, Mote Marine Laboratory, 1600 Ken Thompson Parkway, Sarasota, FL 34236, USA

E-mail: alang@eng.ua.edu


Received 20 March 2014, revised 21 May 2014

Accepted for publication 5 June 2014

Published 21 July 2014

Abstract

Shark scales on fast-swimming sharks have been shown to be movable to angles in excess of 50°, and we hypothesize that this characteristic gives this shark skin a preferred flow direction. During the onset of separation, flow reversal is initiated close to the surface. However, the movable scales would be actuated by the reversed flow thereby causing a greater resistance to any further flow reversal and this mechanism would disrupt the process leading to eventual flow separation. Here we report for the first time experimental evidence of the separation control capability of real shark skin through water tunnel testing. Using skin samples from a shortfin mako *Isurus oxyrinchus*, we tested a pectoral fin and flank skin attached to a NACA 4412 hydrofoil and separation control was observed in the presence of movable shark scales under certain conditions in both cases. We hypothesize that the scales provide a passive, flow-actuated mechanism acting as a dynamic micro-roughness to control flow separation.

 Online supplementary data available from stacks.iop.org/BB/9/036017/mmedia

Keywords: flow control, shark skin, flow separation, experimental fluid dynamics

1. Introduction

For millions of years organisms have been swimming and flying through fluids, and from an engineer's perspective they may have evolved means to control flow for obvious efficiency. Flow control is considered to be any deviation from a smooth surface which causes the flow to behave differently and with some benefit (e.g. reduced drag, increased lift). Sharks have an evolutionary history dating back over 400 million years during which their skin's placoid scales have evolved to serve a variety of purposes, including mechanical and biological protection, protection against parasites, anti-fouling, hydrodynamic drag reduction and even bioluminescence [1–4]. The shortfin mako *Isurus oxyrinchus*, perhaps

the fastest swimming shark, has a streamlined, fusiform profile to minimize drag and is known for its speed and agility [5, 6]. Sharks' placoid scales vary in size and shape both by species and by body location on an individual animal, but fast-swimming sharks such as the shortfin mako have evolved some of the smallest scales with crown lengths on the order of 200 μm [7] (figure 1(A)).

Because of their unique skin structure and high swimming speeds, sharks have been studied for several decades to elucidate potential flow control mechanisms that can lead to drag reduction [3, 8–14]. However, the primary focus in the past has been the study of riblets, streamwise ridges on the top of each scale, which are believed to decrease turbulent skin friction drag. Skin friction drag is the sum total of viscous

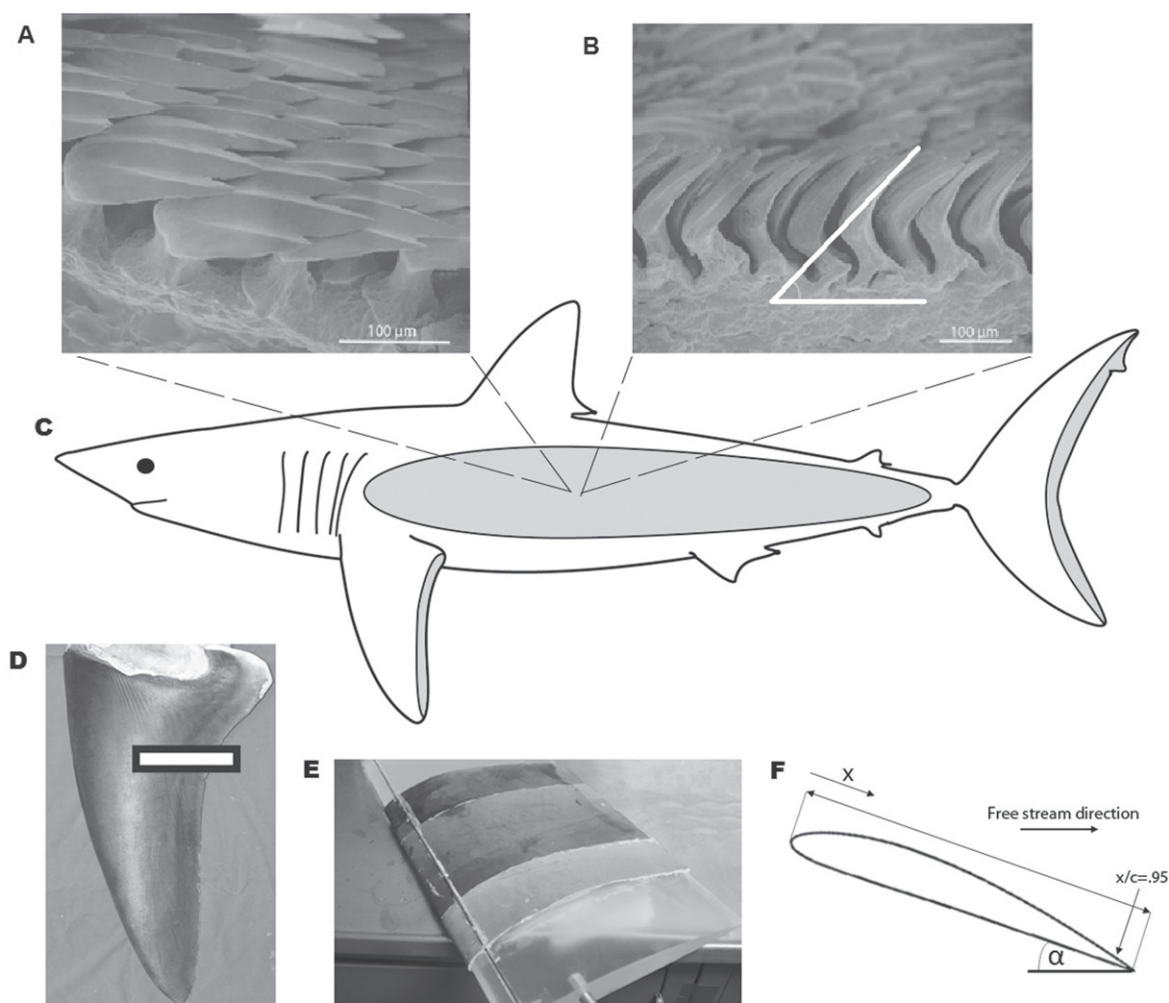


Figure 1. Shark skin images and samples used. (A) SEM (images obtained using a scanning electron microscope) of shark skin scales from the flank region of a shortfin mako *Isurus oxyrinchus*. This view shows the scales from a lateral view and unbristled. (B) SEM of flank scales, lateral view and the white angled line shows in this case they have been manually bristled to approximately 45°. (C) Outline of a shortfin mako shark. Shaded areas designate approximate region on the skin where scales are known to erect in excess of 50°. This figure was redrawn and edited from Motta *et al* 2012. (D) The shortfin mako pectoral fin used for testing. Line shows location of the laser sheet for flow measurements. (E) NACA 4412 hydrofoil with shark skin sample covering 50% of the top surface. Trip wire located at $x/c=0.05$ is visible. (F) Sketch of a NACA 4412 hydrofoil at angle of attack (α) defining downstream distance from the leading edge (x) and chord (c). The location $x/c=0.95$ is designated where local flow velocity was analyzed in figure 5.

shear force from the fluid moving over the skin that has a net component in the direction opposing forward motion of the body. More recent work has focused on the potential for individual scales to be moveable and thus capable of interacting dynamically with the flow [7–9]; in particular it has been found that shortfin mako scales can be manually bristled on dead specimens to angles in the vicinity of 50° and upon release will slowly settle back in place [7]. Figure 1(C) shows the shaded region on the flank where this high bristling capability has been observed. Pressure drag, caused by flow separation, is the net summation of pressure forces acting on the body that opposes the direction of motion. It is speculated that these moveable scales can control flow separation, and would work in a manner similar to dimples on a golf ball, to reduce the size of the viscous wake and thereby reduce pressure drag.

An early hypothesis of shark skin separation control suggested that bristled scales would act as vortex generators [3]. Vortex generators protrude into the flow and are placed upstream of the location where separation needs to be controlled [15]. The vortex generator works by stirring up the flow downstream near the skin thereby transferring higher momentum fluid closer to the wall to inhibit flow separation. However, for scales to protrude up into the flow they must be actuated and, since localized active control of individual scales by the shark is highly unfeasible, the flow itself must provide passive scale actuation and erection via flow reversal. Therefore, the purpose of this new line of research is to investigate the control of flow separation as a result of scale movability, which for the shark would decrease pressure drag leading to increased agility [3].

Flow separation is a viscous flow phenomenon that occurs due to the formation of boundary layers. The onset of flow separation from a surface such as the body of a shark involves a patch of low momentum fluid, near the wall and within the boundary layer, being induced to reverse direction when compared to the main flow due to the presence of a suction pressure located upstream. For instance, on a shark the lowest static pressure typically occurs at the point of maximum girth (gill location) and thus locations posterior to the gills on the flank region would be prone to flow separation. For unsteady flows, flow separation is a process that develops very suddenly (over small time scales) and adjacent to the surface at very small spatial scales [16, 17]. This patch of fluid expands in the streamwise direction while also thickening vertically. As it moves upstream it also gains momentum until instability is reached such that an eruptive plume of boundary layer flow is ejected out from the wall. The eruptive plume, often leading to large scale vortex formation, is what characterizes global flow separation of the flow from the body resulting in high pressure drag [18]. During this process, flow reversal close to the surface can easily exceed 30% of the free stream flow as will be shown in the results presented. In the case of steady laminar flow, the separation point is fairly well defined by a spanwise line of flow detachment. However in the case of a turbulent boundary layer, three-dimensional patches of reversed flow move upstream and downstream unpredictably within the buffer layer (bottom 1% of the boundary layer) and at various spanwise locations. Thus, from a time-averaged sense, the point of separation is defined as the point where 50% of the time the flow is reversed. This measure of the percentage of time that flow is reversed is defined as the backflow coefficient [19].

It should be noted here that for a shark swimming at 10 m s^{-1} the boundary layer is expected to transition from laminar to turbulent at a downstream distance of $x \sim 5 \text{ cm}$; thus the flow over the flank, and over the back portion of the fin where flow separation would be initiated, is most likely turbulent. In the case of a turbulent boundary layer, we propose that thin patches of reversed fluid develop within the low speed streaks [20]; this is the region of lowest momentum that has been lifted up from the wall and is thus most susceptible to the presence of an adverse pressure gradient. This flow reversal near the surface initiates scale bristling which leads to the control of flow separation. Note, this scale actuation is initiated within the region of flow separation for the shark (not upstream of separation) and the formation of cavities between the erected scales (see figure 1(B)) may result in localized momentum exchange with the outer flow due to induced mixing [21]. This mixing would bring high momentum fluid towards the skin as a further mechanism to maintain attached flow.

The purpose of the present study was not necessarily to prove this aforementioned hypothesized flow control mechanism, but rather to demonstrate that shark skin with movable scales can lead to the management of flow separation under controlled experimental conditions, and in particular where the skin is placed on a static (non-deforming) model.

Sharks obviously bend their body whereby this motion leads to the production of thrust and consequent forward swimming. However, static testing of shark skin with positive results validates the presence of a potential separation control mechanism, working at the microscale level on the skin, that could be applied in engineering applications where surfaces are fixed in shape or not moving (e.g. aircraft control surfaces and helicopter rotor blades). In particular, this potentially transformative discovery of a new flow control mechanism, attributed to the presence of a passive, flow-actuated, dynamic roughness which involves sub-millimeter sized roughness elements interacting with the flow at the surface, may lead to bio-inspired engineering applications in numerous scenarios where flow separation is detrimental to performance.

2. Methods

2.1. Imaging of scale bristling

A small sample of shortfin mako skin from the flank was glued to a plate and submerged vertically in a tank, with the skin approximately 1 cm from the glass wall. This permitted visualization of scale movement due to a small jet flow of water directed in the reversed flow direction over the scales. A Nikon D700 camera equipped with a bellows and reversed 17 mm lens placed close to the tank wall permitted the imaging of the scales with sufficient depth of field to discern scale movement. In addition, Alizarin Red stain was used to dye the transparent scales to increase their visibility. A pulsating jet (diameter 1 mm, jet exit about the size of 5–6 scales) with a maximum exit velocity of approximately 10 m s^{-1} , was placed in the near vicinity of the scales. Due to mixing with the ambient water, the core jet velocity decreases quickly from the jet exit and, according to published data on pulsating jets in a similar Re range [22], within 1 cm (10 jet diameters) of the exit the peak velocity would reduce to approximately 5 m s^{-1} . Since the jet exit was also located above the surface (with flow moving parallel to it and the jet piping did not touch the skin), it is difficult to estimate the exact flow velocity that was induced on the scales themselves which resulted in scale bristling. However a good estimate for this setup is in the $2\text{--}5 \text{ m s}^{-1}$ range which in this case caused extreme bristling.

2.2. Shark skin specimens for testing separation control

Water tunnel testing was carried out on two different specimens to observe flow separation under static conditions. First, a left pectoral fin was taken from a shortfin mako and placed vertically within the water tunnel (figure 1(D)). Secondly, a NACA 4412 hydrofoil shape was chosen based on its known separation characteristics. This hydrofoil produces separation occurring around an angle of attack (α) equal to 10° in the vicinity of the trailing edge, and as α is increased the separated region moves upstream such that by 16° and 18° the flow is fully separated over the upper surface [23]. The shortfin mako skin mounted on the hydrofoil was taken from

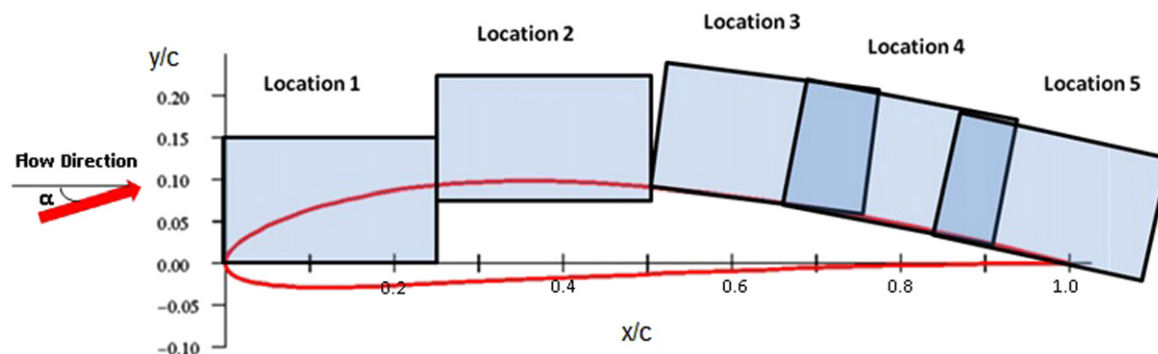


Figure 2. Sketch of NACA 4412 hydrofoil with coordinate system defined and showing all locations at which the flow over the top surface of the hydrofoil was mapped.

the flank of the body posterior to the gills where the most flexible scales are found [7] (capable of erecting to angles of at least 50° , figure 1(B)). The boundary layer over the flank region behind the gills is undoubtedly turbulent ($Re_x \sim 10^7$) and experiences an adverse pressure gradient (maximum girth is located at the gills). As mentioned earlier, it is this area on the shark where flow separation control is of potential importance to a thunniform swimmer such as the shortfin mako.

The mounting process of the shark skin to the hydrofoil (using cyanoacrylate glue) involved removing all excess muscle tissue from the skin while maintaining the dermis to ensure all scales remained undamaged and anchored within the skin. The entire model (chord = 30.5 cm, a width of 61.0 cm was used to span the whole height of the test section and ensure two-dimensional flow) could not be covered with shark skin due to the large surface area. However, three flank skin sections (posterior to the gills and ventral to the dorsal fin), each measuring 33 cm in length with the proper orientation of scales, were used. The middle section mounted at the center was 15.2 cm in width, and two adjacent sections of 7.6 cm width were mounted above and below. Thus the total area covered was 50% of the top surface of the model (figure 1(E)), and the extra length was used to wrap the skin around the leading edge. Once the shark skin was attached to the model, the entire hydrofoil was placed into a freezer to prevent any deterioration of the skin between experiments. Finally, to remove the bristling effect of the scales for the pectoral fin experiment the surface was painted over with latex paint which coated the scales and filled in all the crevices. The paint remained dried onto the skin during the experiments.

2.3. Water tunnel testing

While water tunnel testing of the real skin could not occur at potential burst shark swimming speeds ($\sim 10 \text{ m s}^{-1}$) we hoped the mechanism would be somewhat *Re*-independent; results indicate the threshold backflow required to move the scales and initiate flow control was just reached in some of the experiments. We used a custom-built water tunnel (Eidetics 1520-EXT) with a maximum flow speed of 0.5 m s^{-1} . A time-resolved digital particle image velocimetry (TR-DPIV)

system was used to measure the flow field in a plane perpendicular to the surface and oriented with the flow near the trailing edge. This system uses a pulsed solid-state laser (Quantronix Nd:YLF, 532 nm), high speed CCD camera (Basler A504k, 1280×1024 resolution, running at 500 fps), and TSI Insight 3 G DPIV processing software which uses techniques to decrease measurement error such as local vector validation and image background removal. This processing method also accurately measured flow velocity in the reversing direction and assigned it a negative value. All velocity data were assumed to have been obtained with an error estimate of 5% as is regularly assumed for most DPIV measurements [24] where care was taken to insure correct seeding density and image quality. The data were time-averaged over 2.2 s (1100 image pairs) to quantify flow separation. All models were mounted vertically in the test section with the CCD camera looking from below to focus in on the illuminated seeding particles ($15 \mu\text{m}$ hollow, silver coated glass spheres) within the laser sheet. To increase resolution of the flow measurements, imaging areas were reduced in size. Data were obtained in the case of the hydrofoil over five locations (figure 2), but for the purposes of quantifying flow separation and presenting the data to explain our results, only location 5 at the trailing edge was used for most of the data presentation. In the case of the hydrofoil, data were compared to a second smooth NACA 4412 model with no skin and the boundary layer was tripped in both cases using a 2 mm wire located at $x/c = 0.05$ (figure 1(E)) to better replicate unsteady, turbulent boundary layer conditions.

3. Results

3.1. Visualization of scale bristling by reversed flow

Shortfin mako scales are extremely small and also translucent, making it particularly difficult to visualize scale bristling during the water tunnel studies. However, to document the movability of the scales due only to the presence of water flow in the reversed flow direction a special test was conducted. As described, a small jet of pulsating water passing over a piece of mako flank skin submerged in a tank induced scale bristling (figure 3 and movie in supplementary

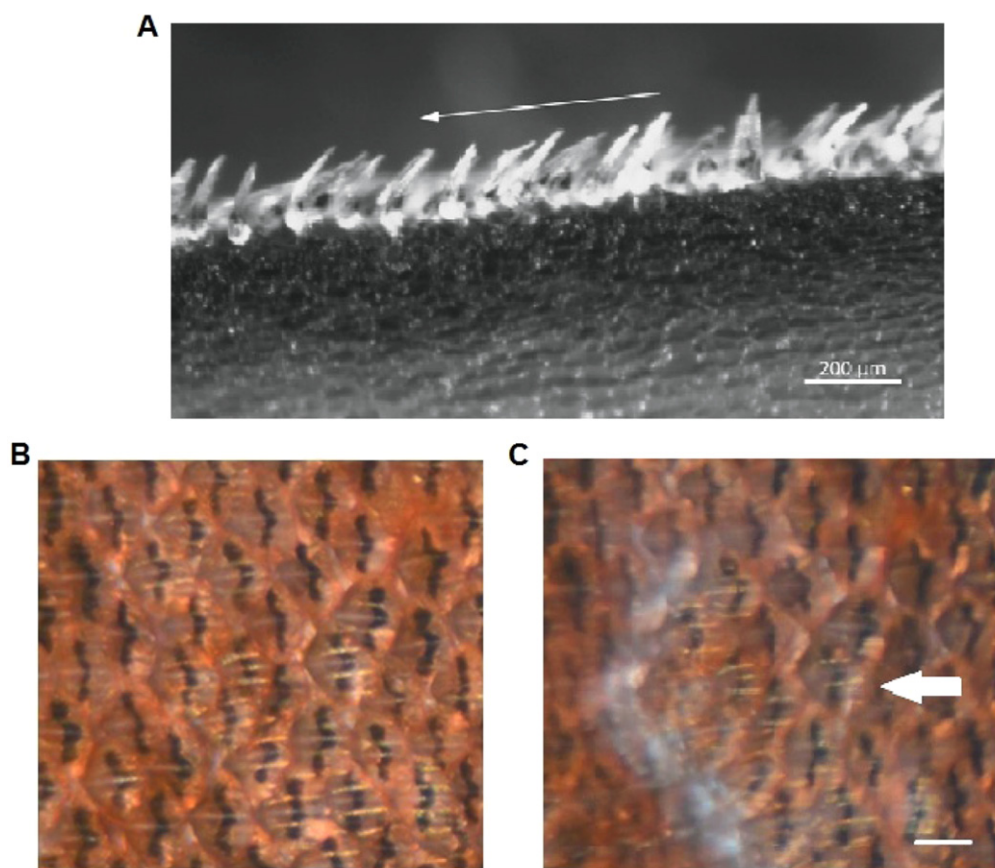


Figure 3. (A) Light microscopy image of manually bristled flank scales from a shortfin mako *Isurus oxyrinchus*. The scales are viewed from a lateral perspective showing the translucency of the scales. Arrow shows direction of flow reversal that will actuate bristling of the scales. (B) Shark scales dyed red, viewed from above, and laying flat as in figure 1(A). (C) Jet flow passing over the scales from right to left, indicated by the arrow, has caused an approximate vertical row of scales to bristle when compared to the unbristled case in (B). The white region indicates the white-colored skin underneath the scales that is now visible due to the localized bristling by the jet flow. The images in (B) and (C) are snapshots from a video which clearly shows scales being actuated up and down due to the presence or absence of the jet flow. See supplementary information to watch the video. Scale bars provided in (A) and (C) are approximate with a value of $200\ \mu\text{m}$ in length.

information). This indicates that the erection of the scales is possible by water flow reversal alone and does not necessitate body undulation or any active mechanism to cause the scales to bristle. Therefore, the shark skin surface has the capability to act as a passive, flow-actuated dynamic micro-roughness. We hypothesize that it is this mechanism, whereby the surface has a preferred flow direction such that flow reversal induces scale bristling, which results in separation flow control.

3.2. Laminar separation control over a pectoral fin

The flow over a shortfin mako pectoral fin, at a location about one-third of the total span from the base of the fin and covering the following one-third of the trailing edge, was studied. This location (at a chord of 13.6 cm) was chosen because the flow became more three-dimensional as the tip of the tapered fin was approached (see figure 1(D)). The shape of the cross-section of the fin at the location tested was traced and found to most closely agree with that of a NACA 4510 airfoil. By this designation, the fin has 4% camber with maximum camber located at 50% of the chord. The maximum thickness of the fin is 10% of the chord. It should be noted that the scale

flexibility varies over the fin surface, with the highest bristling capability at the trailing edge with a measured angle of 32° ; flexibility then lowers slightly at mid-chord to 23° all the way to zero at the leading edge [7]. We propose that scale movability is used as a means to manage flow separation over the fin to maintain its use as a control surface for the shark during high speed turning maneuvers.

Two flow speeds were tested with the pectoral fin ($U = 32$ and $50\ \text{cm s}^{-1}$, $Re_c = 5.5 \times 10^4$ and 8.6×10^4) and the tests were conducted at various angles of attack (α) between 0 and 12° . In this case the boundary layer flow was laminar, although unsteadiness in the flow can be attributed to vortex formation within the separated shear layer for cases where flow separation was observed. The most interesting results occurred at the highest angle of attack that was tested, $\alpha = 12^\circ$ (figure 4). Plotting contours of backflow coefficient, or the percentage of time during which the flow is reversed (a direct measure of the level of flow separation [19]), reveals that at the higher flow speed almost complete control of the flow separation was maintained with the presence of the scales (figure 4(B)). As flow speed is increased, higher backflow velocities will also result near the surface. We thus suggest

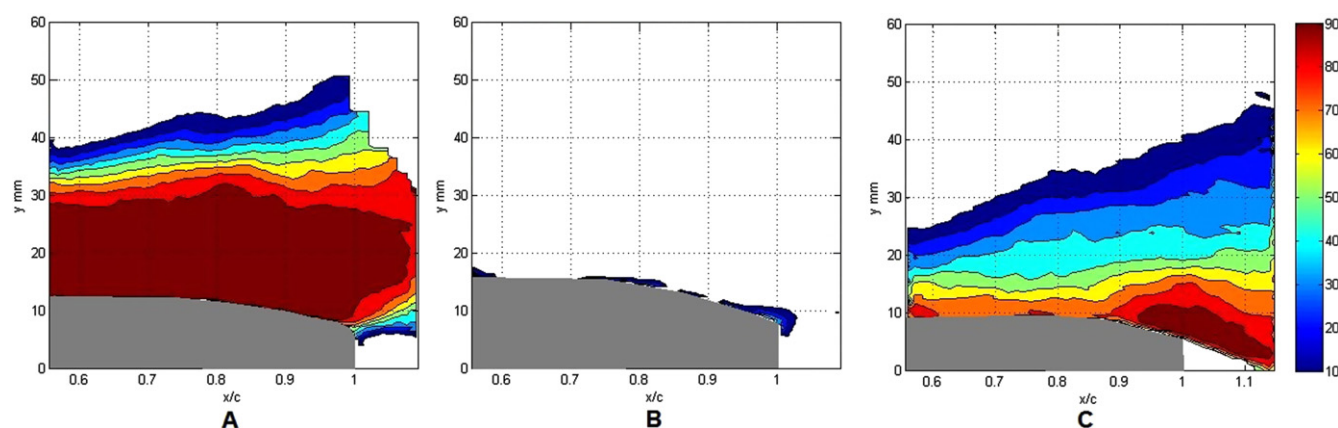


Figure 4. Time-averaged DPIV contour plots of back flow coefficient (percentage of time that flow is reversed at any particular location regardless of flow magnitude) for flow over the pectoral fin of a shortfin mako *Isurus oxyrinchus* (figure 1(D)) at $\alpha = 12^\circ$. (A) Fin with scales intact, $U = 32 \text{ cm s}^{-1}$. (B) Fin with scales intact, $U = 50 \text{ cm s}^{-1}$. (C) Fin with scales painted over to remove their flow control effect, $U = 50 \text{ cm s}^{-1}$. The very low levels of backflow in case (B) indicates that flow separation was controlled for this case, but not cases (A) and (C) where backflow levels are very high and often exceeding 90%.

that the difference in results based solely on flow speed tested is due to a potential threshold of reversed shear flow that is required to initiate scale bristling, and that this threshold was surpassed in the higher Re case. This hypothesis is further corroborated by the next set of experiments conducted over the hydrofoil. Finally, when the scales were painted over, preventing their bristling, and the model placed back into the tunnel at the same flow speed and angle of attack, flow separation was again present over the fin (figure 4(C)).

3.3. Turbulent separation control over a shark skin covered hydrofoil

Flow was measured at center span of a NACA 4412 hydrofoil model for six angles of attack ($\alpha = 8^\circ, 10^\circ, 12^\circ, 14^\circ, 16^\circ$ and 18°) at a speed of 32 cm s^{-1} ($Re_c = 1 \times 10^5$). On the smooth hydrofoil at the lowest value of $\alpha = 8^\circ$, the flow began exhibiting a backflow coefficient of 20% at the more upstream position of $x/c = 0.974$ (see figure 1(F) for coordinate definitions). By a value of $\alpha = 12^\circ$, the first appearance of turbulent boundary layer separation (backflow coefficient = 50%) occurred at $x/c = 0.941$, and by 16° this location moved forward to $x/c = 0.719$. In comparison with the shark skin case at the lower angles of attack the skin had a negative effect on the flow. At 8° a backflow coefficient of 20% was located at $x/c = 0.948$, and 50% backflow first occurred at a lower angle of 10° at $x/c = 0.983$. It was not until $\alpha = 16^\circ$ that the flow control of the shark scales began to take effect with a 50% backflow coefficient now located at $x/c = 0.795$ (this point moved downstream by 8% chord compared to the smooth case). But most importantly, at 18° the flow separation was almost completely controlled (figure 5). We deduced that at the lower angles of attack the reversing flow was of insufficient strength to activate the scales, and the additional thickness of the skin added to the hydrofoil model had a negative effect on its performance. However, as the angle of attack increased, the reversing flow increased in magnitude and by 16° there were patches of reversed flow with sufficient strength to bristle the

scales such that for a certain percentage of time the flow was controlled. At $\alpha = 18^\circ$, the reversed flow magnitudes increased for the smooth case, and with a greater amount of scale bristling likely to occur the flow was almost fully controlled. Figure 6 shows the full capture of the separated flow region at $\alpha = 16^\circ$ for both the smooth and shark skin surface hydrofoils. Finally, it should be noted that the gray regions in figures 4–6 do not accurately show the shape of the fin or hydrofoil but indicate the regions where the laser light was physically blocked by the model such that the upper edge does represent the fin or hydrofoil surface.

To better understand the localized effect on the velocity near the surface of the skin, time traces of flow velocity at $x/c = 0.95$ and located 5 mm above the surface were analyzed (as extracted from the previous experimental data) with variation in angle of attack for the hydrofoil (figure 7). At 12° , one can make two observations. The smooth case evidenced a higher frequency of fluctuation between forward and reversed flow and only twice did the reversed flow velocity exceed 20 cm s^{-1} . For the shark skin case the flow appeared to remain reversed for longer periods of time. At 16° , the flow control of the scales was beginning to take effect; for the smooth case the flow appeared to have longer time periods of reversed flow and the reversed flow was larger in magnitude (regularly exceeding 10 cm s^{-1} or 30% of the freestream velocity). Finally at 18° the smooth case had reversed flow over 90% of the time, and the reversed flow magnitude regularly exceeded 20 cm s^{-1} . In the shark skin case it appears that flow reversal is virtually stopped and for the few incidents where flow reversal occurred it rarely exceeded 20 cm s^{-1} .

4. Discussion

These results should be considered with respect to the bristling angle, and thus actuation height, of the shark scales within a boundary layer of a certain thickness (δ) achieved in the experiments. Here we consider simple flat plate boundary

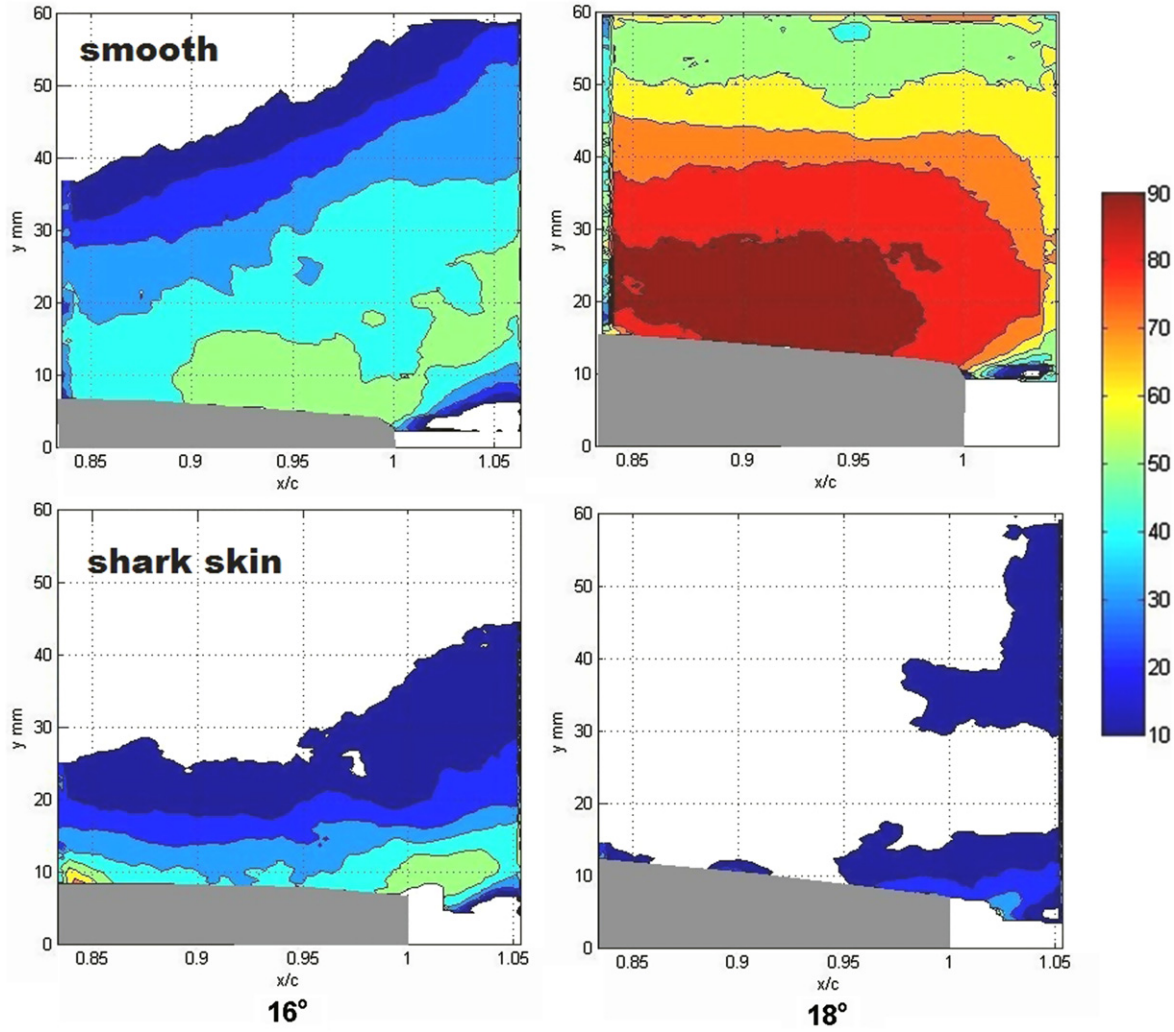


Figure 5. Time-averaged DPIV contour plots of back flow coefficient (e.g. 90 indicates 90% of the time that the flow is reversed at that location) for flow in the vicinity of the trailing edge of a NACA 4412 hydrofoil covered with flank skin from a shortfin mako *Isurus oxyrinchus* (figures 1(E) and (F)) for $\alpha = 16^\circ$ and 18° . Top plots are for a smooth surface, bottom plots are a surface covered with shark skin. $U = 32 \text{ cm s}^{-1}$, $Re_c = 1 \times 10^5$. This demonstrates that as α is increased into a region where flow separation for a smooth surface is known to be present, the shark skin is able to control it and in the 18° case flow separation is almost completely controlled.

layer approximations for all cases to calculate laminar (equation (1)) or turbulent boundary layer thickness (equation (2)) as a function of x (distance along the body), and we acknowledge that these estimates do not account for a variation in boundary layer thickness due to the effect of a pressure gradient due to body curvature but in fact serve as first order estimates.

$$\delta_{\text{lam}} = \frac{5x}{\sqrt{Re_x}}, \quad (1)$$

$$\delta_{\text{turb}} = \frac{0.16x}{Re_x^{1/7}}. \quad (2)$$

In the case of the pectoral fin experiments, the boundary layer is assumed to be laminar prior to separation ($Re_x < 5 \times 10^5$). At mid-chord the boundary layer thickness (δ) would measure approximately 1.3 mm to as large as 2.6 mm if it remains attached all the way to the trailing edge (as in the case where $Re_x = 8.6 \times 10^4$). The shark scales at the trailing

edge are capable of bristling to about 32° and have a crown length in the vicinity of $191 \mu\text{m}$ [7]. Using trigonometry of a bristled scale as in figure 2(A), an approximate estimate would have a single scale upon actuation protruding up within the boundary layer about 0.1 mm (total boundary layer thickness of 2.6 mm). Therefore, this actuation would occur within the lower 5% of the boundary layer thickness.

Similarly, we now consider the case of the hydrofoil with a tripped boundary layer at $Re_x = 1 \times 10^5$. At the trailing edge the boundary layer, when attached, would have an approximate thickness of $\delta = 9 \text{ mm}$. The scales from the flank region have a crown length of $220 \mu\text{m}$ with a bristling capability of 48° and thus would protrude up into the boundary layer approximately 0.16 mm. Therefore, this actuation would occur within the lower 2% of the boundary layer thickness. However, considering the fact that the viscous sublayer and buffer zone, where fundamental turbulent production is considered to occur within the turbulent boundary layer, nominally are located in the bottom 1% of the boundary layer,

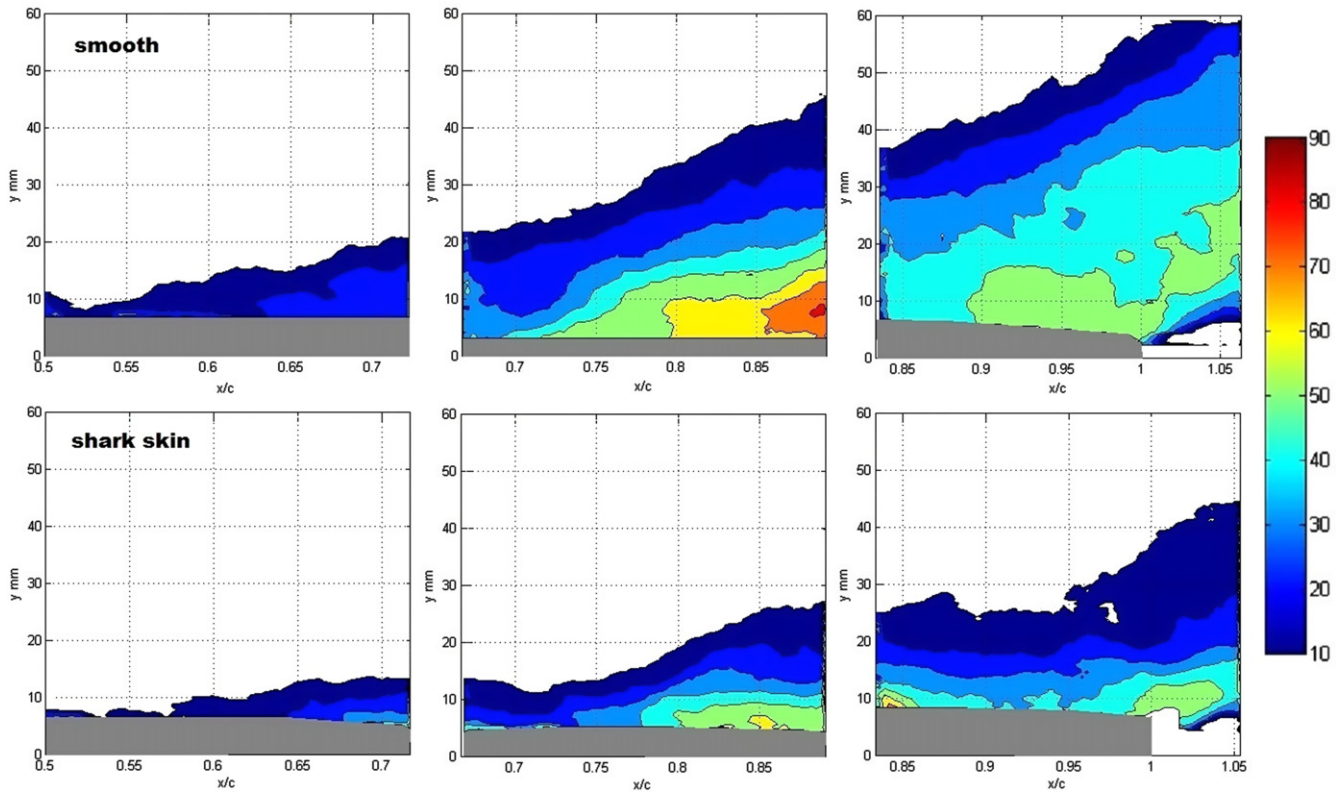


Figure 6. Time-averaged backflow coefficient contours showing the entire flow separation region over the hydrofoil at $\alpha = 16^\circ$ over locations 3–5. (Top) Smooth case. (Bottom) Shark skin covering the surface.

these scales are in fact capable of interacting with the near wall patches of flow reversal within the low speed streaks that would occur in this region.

Finally, consider these same length scales for the case of a shark swimming at 10 m s^{-1} . At a flank location of $x = 1 \text{ m}$ from the nose, a simple estimate gives $Re_x = 1 \times 10^7$. For the case of a pectoral fin, a trailing edge location again of $x = 13.6 \text{ cm}$ from the leading edge would result in a $Re_x = 1.4 \times 10^6$. A turbulent boundary layer at $x = 1 \text{ m}$ would have an approximate thickness of $\delta = 1.5 \text{ cm}$, while the boundary layer at the fin trailing edge would have $\delta = 3 \text{ mm}$. Thus for the pectoral fin a scale protruding up $100 \mu\text{m}$ would reach into the lower 3% of the boundary layer and thus well into the buffer layer. On the flank region where bristling angles are larger, a scale protruding $160 \mu\text{m}$ would just reach into the lower 1% as required to interact with the buffer layer. Bernard & Wallace [25] proposed that the buffer layer is considered to be home to the most interesting dynamical processes with the turbulent boundary layer flow field. As such, roughness elements which penetrate into this region of the flow could certainly control key flow developments. While these estimates are approximate, it is interesting to note how closely the experimental conditions match to the conditions on a shark (within a factor of about 2) such that in both cases the scales are adequately sized to protrude up into the flow upon actuation.

The above discussion clearly demonstrates the ability of the scales to protrude with sufficient height into the boundary layer to affect and impede reversing flow in both the

experiments and for swimming sharks; therefore the first proposed mechanism has the potential to be present in both cases that were tested experimentally. However upon bristling, the scales result in the presence of cavities within the boundary layer and the mixing induced by these cavities is highly dependent on the cavity Reynolds number (Re_c , based on freestream flow and scale height). For a shark swimming at 10 m s^{-1} with a crown length of $220 \mu\text{m}$ on an individual scale, the resulting Re_c would have a value of 2200. In the experiments with a freestream speed of 32 cm s^{-1} the Re_c is reduced to 70. It is surmised that this large difference in Re_c could suggest that the real shark skin would induce much larger levels of mixing due to instabilities within the cavity flow [8] itself for the higher Re_c case. Therefore, the effectiveness of the real shark skin to control the flow separation *in the experiments* may have been hampered due to a reduction in the mixing enhancement, within the boundary layer by the presence of the cavities formed between bristled shark scales, because of the lower Re . We therefore hypothesize that the separation control effectiveness of the real shark skin may in fact be greater for the shark than what was observed.

5. Conclusions

First, we conclude that shark skin found on the flank and pectoral fins of a mako shark is capable of controlling flow separation. These results, achieved for two different experiments (laminar and turbulent boundary layers) and for two

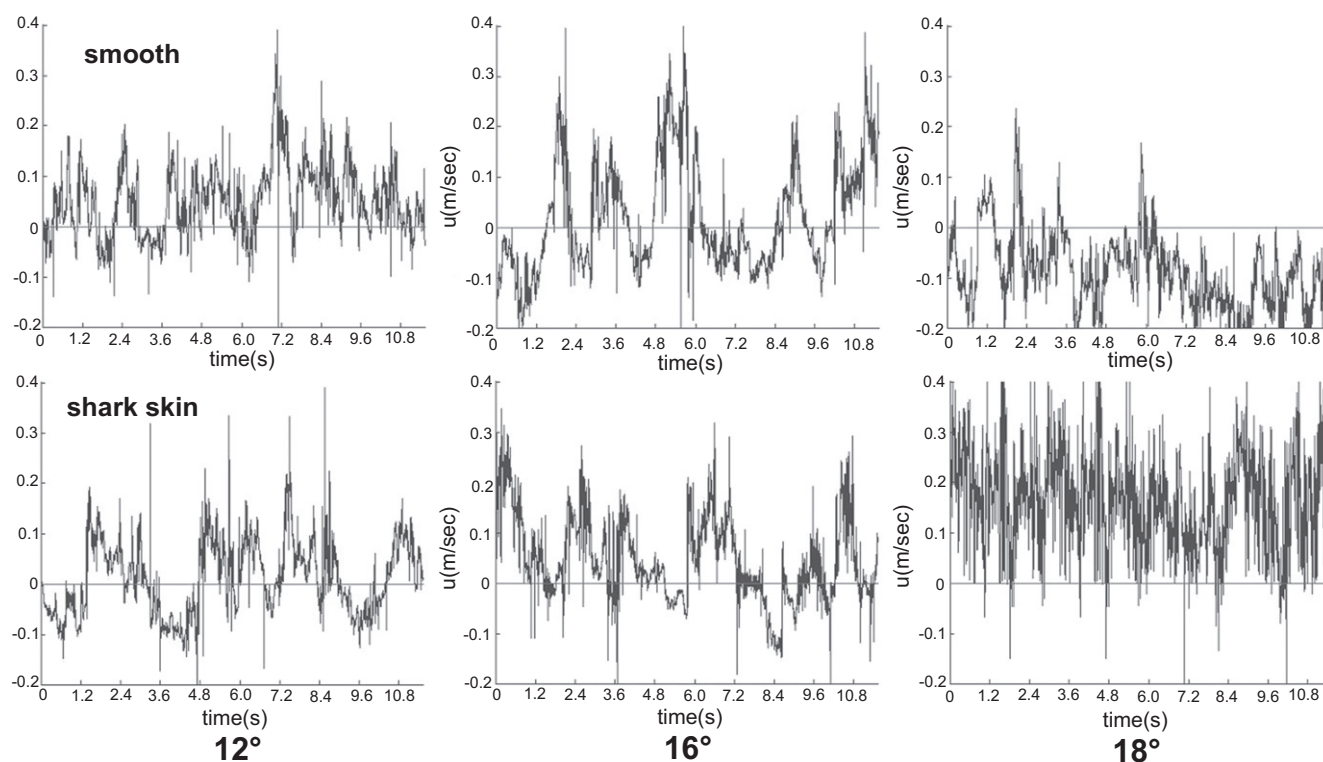


Figure 7. Time traces of x -component of flow velocity at $x/c=0.95$ (figure 1(F)) at a location approximately 5 mm above the surface of a smooth flat plate (above) and the surface covered with flank skin and scales from a shortfin mako *Isurus oxyrinchus* (below). Velocities above zero indicate forward flow, whereas negative values indicate reversed flow over the surface. $U = 32 \text{ cm s}^{-1}$, $Re_c = 1 \times 10^5$. This demonstrates that as α is increased, the flow over the smooth surfaces experiences larger flow reversal magnitudes. However, these results show that flow reversal is largely absent in the 18° case over the shark skin, suggesting that the movability of the scales inhibited flow reversal and controlled flow separation.

different samples of shark skin from key locations on the body, confirm our hypothesis that shark scales act as a means of controlling flow separation. Secondly, our observations indicate that at the higher angles of attack, or at the higher flow speed for the pectoral fin case, flow reversal velocities induced in our experiments were of sufficient strength to induce a separation control mechanism likely due to the movability of the shark scales. For a shark swimming at 10–30 times faster than these experiments, this threshold would be achieved an even greater percentage of the time for highly effective flow control. Third, since flow control during experimental runs with lower reversed flow speeds was not observed, and the fact that scales with greater flexibility correspond to body locations where separation control is more important [7], we have partially confirmed our hypothesis that sharks have a separation control mechanism that is dependent on scale movability and bristling. Future work plans to measure the occurrence of scale bristling when a flow is controlled to fully confirm this hypothesis.

The benefits for the shark, to have scales capable of controlling flow separation, would include decreased pressure drag and increased maneuverability; these are the driving evolutionary factors that resulted in the appearance of this mechanism within the skin of fast-swimming sharks. It should also be noted that flexible scales are also found on the trailing edge of the caudal fin, which may be beneficially controlling

flow separation for increased thrust production [26, 27]. Our goal for future work is to further elucidate the mechanisms, including the passive flow-actuated bristling of the scales, resulting in flow control through continued hydrodynamic testing and prove the proposed hypothesis for flow control.

Finally, this discovery of a flow control technique can lead to the development of bio-inspired man-made surfaces that can be applied in a wide array of engineering applications where flow separation is currently detrimental to performance. Wind turbine blades, submarines, and aircraft control surfaces where vortex generators are already in use are just a few examples. One important problem that has been studied for decades is the development of flow separation, and subsequent loss of lift on rotor blades, as flight speed increases for a helicopter, resulting in a limitation on how fast helicopters can fly. This is just one example where the ultimate application of a man-made shark-inspired surface could have a large impact on the flight performance of a vehicle.

Acknowledgments

We gratefully acknowledge the support of NSF (though grants 0932352, 1062611 and 1127613) and the Porter Family Foundation. Any opinions, findings, and conclusions or recommendations expressed in this material are those of

the author(s) and do not necessarily reflect the views of the National Science Foundation. M Bradshaw performed this research using NSF REU support. J Smith was supported by a University of Alabama Graduate Council Fellowship and US Department of Defense (AMRDEC) funding. We are also thankful to Lisa Natanson, Paul and Jane Majeski and crew, Captain Mark Sampson, Captain Al VanWormer, Captain Kevin Deiter, Phil Pegley, Blake Augsburger, Jack Morris and Mote Marine Laboratory for providing or aiding in the acquisition of shark specimens.

References

- [1] Reif W and Dinkelacker A 1982 Hydrodynamics of the squamation in fast swimming sharks *Neues Jahrbuch Geol. Paläontologie Abh.* **164** 184–7
- [2] Raschi W and Tabit C 1992 Functional aspects of placoid scales: a review and update *Aust. J. Mar. Freshwater Res.* **43** 123–47
- [3] Bechert D, Bruse M, Hage W and Meyer R 2000 Fluid mechanics of biological surfaces and their technological application *Naturwissenschaften* **87** 157–71
- [4] Sansom I, Smith M and Smith P 1996 Scales of thelodont and shark-like fishes from the Ordovician of Colorado *Nature* **379** 628–30
- [5] Carey F and Teal J 1969 Mako and Porbeagle: warm bodied sharks *Comparative Biochem. Physiol.* **28** 199–204
- [6] Stevens J 2009 *Sharks of the Open Ocean: Biology, Fisheries and Conservation* ed M Camhi, E Pikitch and E Babcock (Oxford: Blackwell) chapter 7 (The Biology and Ecology of the Shortfin Mako Shark, *Isurus Oxyrinchus*) pp 87–94
- [7] Motta P, Habegger M-L, Lang A, Hueter R and Davis J 2012 Scale morphology and flexibility in the shortfin mako *Isurus oxyrinchus* and the blacktip shark *Carcharhinus limbatus* *J. Morphology* **273** 1096–110
- [8] Lang A, Motta P, Hidalgo P and Westcott M 2008 Bristled shark skin: a microgeometry for boundary layer control? *Bioinspir. Biomim.* **3** 1–9
- [9] Lang A, Motta P, Hueter R, Habegger M-L and Afroz F 2011 Shark skin separation control mechanisms *Mar. Technol. Soc. J.* **45** 208–15
- [10] Walsh M 1982 Turbulent boundary layer drag reduction using riblets *AIAA 20th Aerospace Sciences Meeting (Orlando, FL, Jan. 1982)* AIAA-82-0169
- [11] Bushnell D and Moore K 1991 Drag reduction in nature *Ann. Rev. Fluid Mech.* **23** 65–79
- [12] Bechert D, Bruse M, Hage W, Van der Hoeven J and Hoppe G 1997 Experiments on drag-reducing surfaces and their optimization with an adjustable geometry *J. Fluid Mech.* **338** 59–87
- [13] Bechert D, Bruse M and Hage W 2000 Experiments with three-dimensional riblets as an idealized model of the shark skin *Exp. Fluids* **28** 403–12
- [14] Oeffner J and Lauder G 2012 The hydrodynamic function of shark skin and two biomimetic applications *J. Exp. Biol.* **215** 1785–95
- [15] Lin J 2002 Review of research on low-profile vortex generators to control boundary-layer separation *Prog. Aerosp. Sci.* **38** 389–420
- [16] Cassel K, Smith F and Walker J 1996 The onset of instability in unsteady boundary-layer separation *J. Fluid Mech.* **315** 223–56
- [17] Doligalski T, Smith C and Walker J 1994 Vortex interactions with walls *Ann. Rev. Fluid Mech.* **26** 573–616
- [18] Gad-el-Hak M 2000 *Flow Control: Passive, Active, and Reactive Flow Measurement* (Cambridge: Cambridge University Press)
- [19] Simpson R 1997 Aspects of turbulent boundary layer separation *Prog. Aerosp. Sci.* **32** 457–521
- [20] Smith C and Metzler S 1983 The characteristics of low-speed streaks in the near-wall region of a turbulent boundary layer *J. Fluid Mech.* **129** 27–54
- [21] Djenidi L, Anselmet F and Antonia R 1999 The turbulent boundary layer over transverse square cavities *J. Fluid Mech.* **395** 271–94
- [22] Pratomo H and Bremhorst K 2012 Experimental study on the propagation of a pulsed jet *Procedia Eng.* **50** 174–87
- [23] Andino M, Braud C, Glauser M, Higuchi H and van Langen P 2005 Global effects of flow control over a NACA 4412 hydrofoil *35th AIAA Fluid Dynamics Conf. (Toronto, Canada, June 6-9)*
- [24] Huang H, Dabiri D and Gharib M 1997 On errors of digital particle image velocimetry *Meas. Sci. Technol.* **8** 1427–40
- [25] Bernard P and Wallace J 2002 *Turbulent Flow: Analysis, Measurement, and Prediction* 1st Edn (Hoboken, NJ: Wiley) p 111
- [26] Fish F and Lauder G 2013 Not just going with the flow *Am. Sci.* **101** 114–23
- [27] Azuma A 2006 *The Biokinetics of Flying and Swimming* 2nd Edn (Reston, VA: American Institute of Aeronautics and Astronautics) p 331